Observation of a continuous phase transition in a shape-memory alloy

J. C. Lashley,[1] S. M. Shapiro,[2] B. L. Winn,[3] C. P. Opeil,[4] M. E. Manley,[5] A. Alatas,[6] W. Ratcliff,[7]
T. Park,[1,8] R. A. Fisher,[1] B. Mihaila,[1] P. Riseborough,[9] E. K. H. Salje,[10] and J. L. Smith[1]

[1]*Los Alamos National Laboratory, Los Alamos, NM 87545, USA*
[2]*Brookhaven National Laboratory, Upton, NY 11973, USA*
[3]*Oak Ridge National Laboratory, Oak Ridge, TN 37831, USA*
[4]*Boston College, Department of Physics, 140 Commonwealth Avenue, Chestnut Hill, MA 02467, USA*
[5]*Lawrence Livermore National Laboratory, Livermore, CA 94550, USA*
[6]*Advanced Photon Source, Argonne National Laboratory, Argonne, IL 60439, USA*
[7]*National Institute of Standards and Technology, Gaithersburg, MD 20899, USA*
[8]*Department of Physics, Sungkyunkwan University, Suwon 440-746, Korea*
[9]*Department of Physics, Temple University, Philadelphia, PA 19122, USA*
[10]*Department of Earth Sciences, University of Cambridge, Downing Street, Cambridge CB2 3EQ, UK*

Elastic neutron-scattering, inelastic x-ray scattering, specific-heat, and pressure-dependent electrical transport measurements have been made on single crystals of AuZn and $Au_{0.52}Zn_{0.48}$ above and below their martensitic transition temperatures ($T_M = 64$ K and 45 K, respectively). In each composition, elastic neutron scattering detects new commensurate Bragg peaks (modulation) appearing at $Q = (1.33, 0.67, 0)$ at temperatures corresponding to each sample's T_M. Although the new Bragg peaks appear in a discontinuous manner in the $Au_{0.52}Zn_{0.48}$ sample, they appear in a continuous manner in AuZn. Surprising us, the temperature dependence of the AuZn Bragg peak intensity and the specific-heat jump near the transition temperature are in favorable accord with a mean-field approximation. A Landau-theory-based fit to the pressure dependence of the transition temperature suggests the presence of a critical endpoint in the AuZn phase diagram located at $T_M^* = 2.7$ K and $p^* = 3.1$ GPa, with a quantum saturation temperature $\theta_s = 48.3 \pm 3.7$ K.

A class of materials exhibiting martensitic (diffusionless) phase transformations yields properties used in a range of technological applications including implants to increase flow in restricted blood vessels [1], actuators for the treatment of high myopia [2], voltage generators [3], and orthodontic arch-wires [4]. These properties often depend on the history of the material and may allow it to recover its previous shape after deformation, known as the shape-memory effect (SME). It has long been recognized that these transformations are all thermodynamically first order (discontinuous) [5, 6, 7]. Special cases arise when the order parameter is coupled to an external field in a complicated way, leading to a weakly first-order transition [8], which is believed to result from a complicated coupling between strain and order parameter fluctuations. Because shape-memory alloys and other multiferroic materials owe their functionality to complicated cross-field responses between two (or more) pairs of conjugate thermodynamic variables, a description of the free-energy landscape and the ability to predict functionality become one and the same.

Phenomenological descriptions of the martensitic transformation pathway, based on reciprocal space [9] and real space [10] geometries, have established rules to determine relative twin and crystallographic orientations between the austenite (high-temperature) and martensite (low-temperature) modifications. Knowledge of the symmetry breaking allows for a definition of the energetic driving force in terms of the difference in free energies between phases. In the Ginzburg-Landau (GL) approach, the free energy, G, is expressed as a sum of symmetry invariants. In its simplest form, G is approximated by a polynomial expansion in even powers of an order parameter, Q, as $G(Q) = aQ^2 + bQ^4 + cQ^6 + \frac{g}{2}|\nabla Q|^2$. For martensitic transformations, Q is taken to be strain or strain coupled to shuffle (displacements involving quasistatic phonons with fractional commensurate wave vectors with uniform shears [11]). The coefficients a, b, c, and g are material parameters to be determined experimentally or by first principle simulations.

For the majority of shear-induced transformations, the GL expansion captures the essential physics [12, 13], such as constitutive response [14, 15] and the occurrence of anti-phase boundaries [16]. When applied to shape-memory alloys, the presence of intervening (premartensitic) phases [17] presents difficulties for both experiment and theory as to a unique characterization of the order parameter. Further issues have arisen in materials exhibiting quantum mechanical effects in the band structure and strong electron-phonon coupling [18]. The thermodynamic behavior is best explored when no further transitions occur between T_M and 0 K. This effect was recently reported for Fe-doped NiTi, where all thermodynamic parameters could be correlated self-consistently within mean field theory [19]. In order to integrate these cases into GL theory, it is necessary to measure and access each thermodynamic property and infer cross-field couplings of the order parameter. The ability to distin-
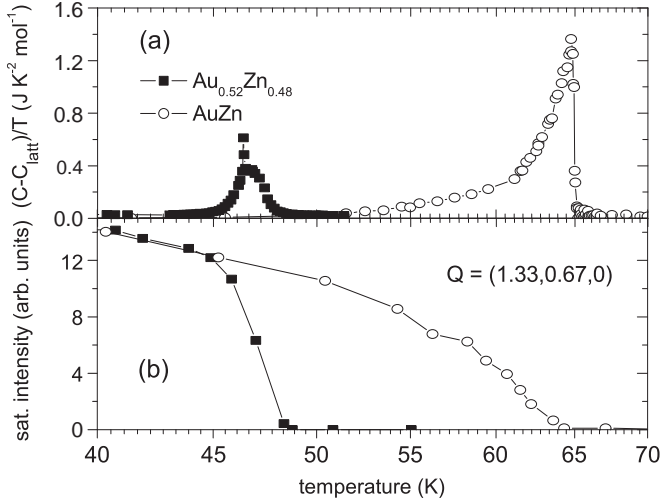
FIG. 1: (a) The excess specific heat divided by temperature versus temperature in the vicinity of the martensitic transitions for $Au_{0.52}Zn_{0.48}$ and AuZn. (b) Temperature dependence of the satellite-peak intensity along $Q = (1.33, 0.67, 0)$. The satellite peak intensity is proportional to the square of the order parameter.

guish subtle differences between first-order and weakly first-order depends on the ability to resolve the behavior of pertinent physical properties.

In this Letter we examine the AuZn system for thermodynamic properties that contribute to the first-order or weakly first-order nature of the free-energy landscape. We measure elastic neutron-scattering, inelastic x-ray scattering, specific-heat, and the pressure dependence of the transition by electrical transport. While we observed classical first-order behavior at 45 K for $Au_{0.52}Zn_{0.48}$, we observed a mean field continuous transformation for AuZn near 64 K in the temperature dependence of the Bragg peak intensity, and a Landau step with a λ anomaly in the excess specific heat.
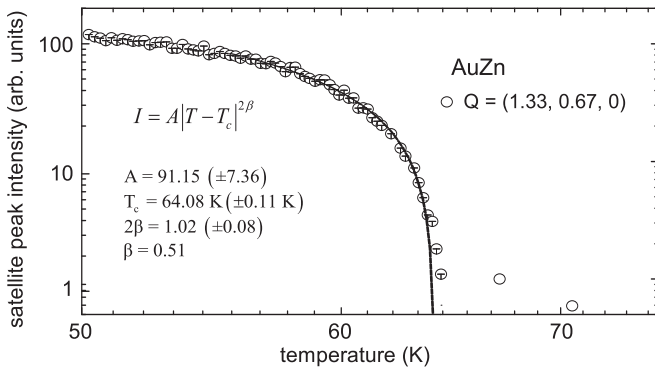

FIG. 2: Temperature dependence of the satellite peak intensity on heating along $Q = (1.33, 0.67, 0)$ in AuZn, near the transition temperature. A fit to mean-field theory for $T \leq T_c$. The points above 64 K are background.
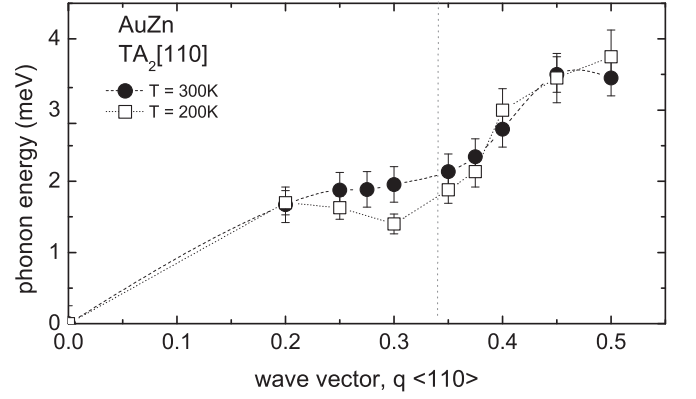

FIG. 3: Temperature dependence of the phonon dispersion in AuZn along the TA_2 branch. At 300 K one notices considerable phonon softening at $q = (0.33, 0.33, 0)$ (vertical line). The dashed lines between points are provided as guides to the eye.

Single crystals were prepared by fusion of the elements in a Bridgman furnace and were oriented by back-reflection Laue diffraction. The neutron experiments were performed on the BT9 triple-axis spectrometer at the NIST research reactor. Measurements of the phonon dispersion were made on XOR of sector 3 at the Advanced Photon Source, Argonne National Laboratory [20, 21]. Specific-heat measurements were measured using a thermal-relaxation calorimeter by Quantum Design [22]. The pressure dependence of the transition temperature was made by a four-terminal ac-transport method in a mechanical pressure cell designed to reach pressures of 3 GPa.

Previous investigations have shown that AuZn exhibits a martensitic transition as seen with low-temperature electron microscopy [23] and by recoverable transformation strain (shape-memory effect) [24]. Figure 1 shows the temperature dependence of (a) the excess specific heat and (b) the satellite peak intensity for $Au_{0.52}Zn_{0.48}$ and AuZn. Although we have measured the specific heat previously [25], it is plotted along with the elastic neutron-scattering data, since it is revealing to compare both sets of measurements that were made on the same samples. We find a latent heat anomaly at 45 K for $Au_{0.52}Zn_{0.48}$. A λ-anomaly was observed for AuZn, but no latent heat was observed. The specific heat near the transition can be influenced by intrinsic defects, including triple-point and anti-structure defects, both known to be present in the B2 structure [26, 27]. It was therefore necessary to use a microscopic probe to determine whether or not the transition could be a broadened first-order transition. Elastic neutron-scattering measurements indicate that in each composition new commensurate Bragg peaks (modulation) appear at $Q = (1.33, 0.67, 0)$ at temperatures corresponding to each sample's T_M Figure 1(b). Mirroring the specific-heat data, the temperature depen-

dence of the satellite peak intensity shows a rapid jump at 45 K in $Au_{0.52}Zn_{0.48}$, while a continuous variation occurs for AuZn on warming starting at 64 K. The satellite peak intensity is proportional to the square of the order parameter, since it leads to the low-temperature rhombohedral phase. The specific-heat data also indicate thermal hysteresis (not shown) of 6 K at 45 K for $Au_{0.52}Zn_{0.48}$. The satellite peak intensity for AuZn depicted in Fig. 1(b) was measured by neutrons on heating and cooling. Unlike the specific-heat data Fig. 1(a) we observe a small discontinuity and 1.5 K difference in transition temperature on cooling.

Figure 2 shows the satellite peak intensity versus temperature in the vicinity of T_M for AuZn. Near the transition temperature, the satellite peak evolves continuously with increasing temperature, showing a temperature dependence given by $I = A|T - T_M|^{2\beta}$; where the satellite peak intensity is I, the critical temperature is T_M, and the critical exponent is β. We obtain T_M=64.08 K $\pm$0.11 K and 2β= 1.02$\pm$0.08. The value of the critical exponent obtained from this fit (β=0.51) is close to the mean-field value of β=0.50 [28]. One could argue that mean-field exponents were obtained by coincidence given that the critical regime, as defined by the Ginzburg-criterion, is restricted to a range of temperatures too small to be resolved by our experiments, or that the correlation length does not diverge, since it is limited by other extrinsic disorder (*i.e.*, martensite twins) or intrinsic fluctuations. The latter possibility seems more

FIG. 5: (a) The electrical-resisitvity data taken on cooling and warming is shown in the vicinity of T_M. (b) Plot of *ln p* versus $1/T$ to test the applicability Clausius-Clapeyron equation.

plausible to us, because the inverse correlation length, or width of the Bragg peaks (not shown), increases as the temperature is lowered below T_M.

As the temperature is lowered, the unit cell is modulated in the [110] shear direction. A commensurate shuffle of every third unit cell results in a hexagonal primitive unit cell formed from nine primitive cubic cells of the parent phase. This structure can also be described in terms of its conventional rhombohedral unit cell. In Fig. 3 we show the TA_2 phonon-dispersion curves along [110], measured by inelastic x-ray scattering at temperatures of 300 K and 200 K. The inflection in the phonon frequency near $\xi = 1/3$ indicates the low shear instability along the TA_2[110] branch. This inflection is comparable to an earlier investigation [29] of off-stoichiometric AuZn samples. At 300 K, the phonon energy positions have been fit over the energy range -4 meV $\leq E \leq$ 4 meV to a double Lorentzian, as shown in Figure 4. The phonons continuously soften with decreasing temperature to the point where separation becomes difficult below 200 K.

Figure 5 (a) shows the change in resistivity between cooling and warming. The data were collected with warming and cooling rates of 0.2 K min^{-1}. In the region of T_M there is no hysteresis, to within experimental error. Because of the lack of hysteresis, we elected to measure the pressure dependence of the transition. For a first-order transition, the Clausius-Clapeyron relation, $\ln p/p_0 = -\Delta H/(RT) + A$, predicts a linear relationship for $\ln p/p_0$ versus $1/T$ with the slope $(-\Delta H/R)$. Here, p denotes the pressure, H the enthalpy, R the universal gas constant, and p_0 is a reference pressure. Figure 5(b) shows the plot of $\ln p$ versus $1/T$. It appears that there is no observable linear region. Assuming that the entropy does not vary significantly with pressure, the conditions for the applicability of the Clausius-Clapeyron relation are not met. This result provides further evidence that
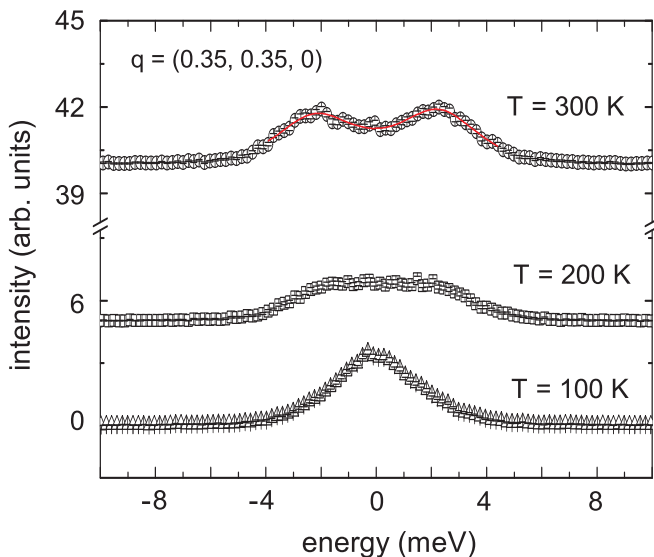

FIG. 4: Inelastic x-ray scattering data showing the temperature dependence near the soft mode, $q = (0.35, 0.35, 0)$. The 300 and 200 K data are offset by 0.004 and 0.0005, respectively on the y-axis for clarity. The energy positions are fit to a double Lorentzian (solid curve) at 300 K to determine the phonon energy. The intrinsic resolution for inelastic x-ray scattering is 2 meV.
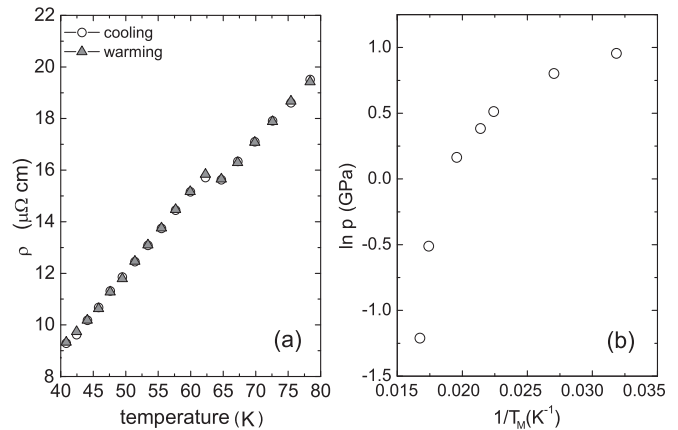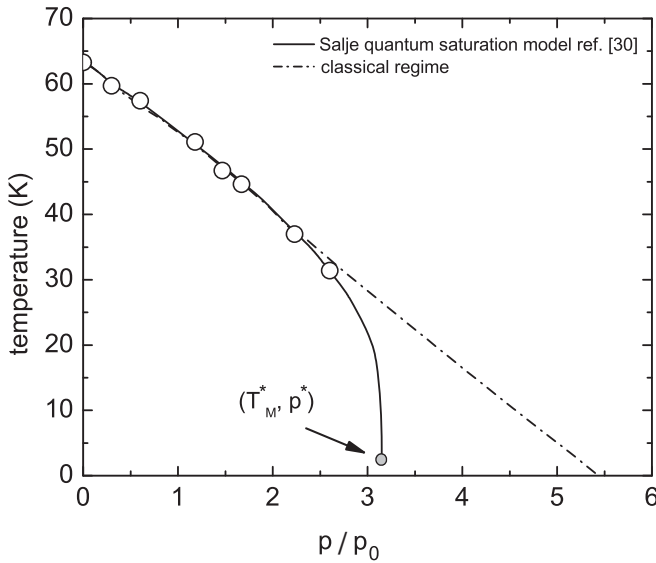
FIG. 6: Pressure dependence of the transition temperature up to pressures of nearly 3 GPa, together with a fit to Salje's model [30] which accounts for quantum saturation effects close to zero absolute temperature. The difference between the linear (classical) and quantum-dominant behavior is illustrated in the inset. We find that quantum effects become important for temperatures lower than $\theta_s = 48.3\pm3.7$ K, and a critical endpoint is predicted at $T_M^* = 2.7$ K and $p^* = 3.1$ GPa.

the transition is not first order.

We use a modified GL free energy expression to describe the quantum saturation in the order parameter expected at sufficiently low temperature [30]. This saturation effect reflects the departure from classical behavior as the absolute temperature approaches zero and is a direct consequence of the third law of thermodynamics. Following Salje *et al.* [30], we fit the pressure dependence of the transition as $\theta_s/T_M(p) = \coth^{-1}\left[\coth(\theta_s/T_M(0)) - p/p_0\right]$. Here θ_s is a phenomenological temperature below which quantum mechanical effects are dominant. We find $p_0 = 5.6\pm0.7$ GPa and $\theta_s=48.3\pm3.7$ K. The resulting phase diagram predicts a critical endpoint at $T_M^* = 2.7$ K and $p^* = 3.1$ GPa. Figure 6 depicts the experimental pressure dependence of the transition temperature for pressures up to nearly 3 GPa, together with the fit to Salje's classical regime. We find a classical slope of -11.7$\pm$0.2 K GPa^{-1}. The difference between the classical and quantum regimes is important for temperatures below θ_s.

In conclusion, we report results of a detailed experimental study of the martensitic transition in AuZn. While the temperature dependence of the satellite peak intensity (proportional to the square of the order parameter) show marked first-order behavior at 45 K for $Au_{0.52}Zn_{0.48}$, we observed a continuous feature well-described by a mean-field exponent (β=0.51) for AuZn at 64 K. This result is contrary to the established definition of a martensitic transition. Providing supporting evidence to the continuous nature of the phase transition in AuZn are the lack of thermal hysteresis from electrical-resistivity measurements, the λ-anomaly in the specific heat, and the disagreement of pressure data with the Clausius-Clapeyron relation. Using Salje's model to describe the quantum saturation effects close to zero absolute temperature, we predict the presence of a critical endpoint in the phase diagram located at $T_M^* = 2.7$ K and $p^* = 3.1$ GPa, with a phenomenological temperature θ_s=48.3$\pm$3.7 K for the onset of quantum effects.

[1] P. W. Duerig, MRS Bulletin **27**, 101 (2002).
[2] I. Yu *et al.*, Mater. Sci. Eng. A **481-482**, 651 (2008).
[3] I. Suorsa *et al.*, J. Appl. Phys. **95**, 8054 (2004).
[4] J. Jafari, S. M. Zebarjad, and S. A. Sajjadi, Mater. Sci. Eng. A. **473**, 42 (2008).
[5] R. C. Albers *et al.*, Comp. and Appl. Math. **23**, 345 (2004).
[6] J. G. Boyd and D. C. Lagoudas, Int. J. Plasticity **12**, 805 (1996).
[7] P. W. Gash, J. Appl. Phys. **54**, 6900 (1983).
[8] S. Rubini and P. Ballone, Phys. Rev. B. **48**, 99, (1993).
[9] J. S. Bowles and J. K. Mackenzie, Act. Met. **2**, 129 (1954).
[10] M. S. Wechsler, D. S. Lieberman, and T. A. Read, J. of Metals **5**, 1503 (1953).
[11] W.G. Burgers, Physica Utrecht **1**, 561 (1934).
[12] P. Toledano and P. Toledano, The Landau Theory of Phase Transformations (World Scientific, Singapore, 1987).
[13] E. K. H. Salje, Phase Transformations in Ferrelastic and Co-elastic Solids (Cambridge University Press, Cambridge, UK, 1990).
[14] R. Ahluwalia *et al.*, Acta. Mat. **52**, 209 (2004).
[15] M. Iwata and Y. Ishibashi, J. Phys. Soc. Jap. **72**, 2843 (2003).
[16] W. Cao, A. Saxena, and D. M. Hatch, Phys. Rev. B. **64**, 024106 (2001).
[17] S. Kartha *et al.*, Phys. Rev. Lett. **67**, 3630 (1991).
[18] K. H. Ahn *et al.*, Phys. Rev. B. **71**, 212102 (2005).
[19] E. K. H. Salje *et al.*, J. Phys. Cond. Matt., **20**, 275216 (2008).
[20] H. Sinn *et al.*, Nucl. Inst. and Meth. in Phys. Res. A **467**, 1545 (2001).
[21] H. Sinn, J. Phys. Cond. Matter **13**, 7525 (2001).
[22] J. C. Lashley *et al.*, Cryogenics **43**, 369 (2003).

[23] H. Pops and T. B. Massalski, Trans. Met. Soc. AIME **223**, 728 (1965).

[24] T. Darling *et al.*, Phil. Mag. B. **82**, 825 (2002).

[25] R. McDonald *et al.*, J. Phys. Cond. Mat. **17**, L69 (2005).

[26] Y. A. Chang and J. P. Neumann, Prog. Sol. St. Chem. **14**, 221 (1985).

[27] D. Gupta and D. S. Lieberman, Phys. Rev. B. **4**, 1070 (1971).

[28] J. J. Binney, N, J, Dowrick, A. J. Fisher, and M. E. J. Newman, Theory of Critical Phenomena (Oxford Science Publications, Oxford University Press Inc., New York, 1993).

[29] T. Makita *et al.*, Phys. B. **213**, 430 (1995).

[30] S. A. Hayward and E. K. H. Salje, J. Phys.: Condens. Matter **10**, 1421 (1998); J. M. Pérez-Mato and E. K. H. Salje, *ibid.* **12**, L29 (2000).